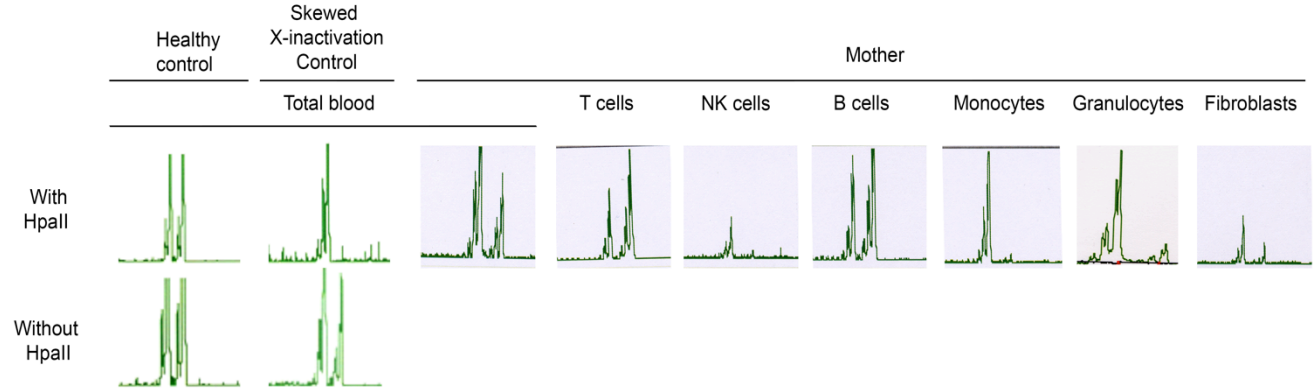


Supplementary data

Rescue of recurrent deep intronic mutation underlying cell type-dependent quantitative NEMO deficiency.

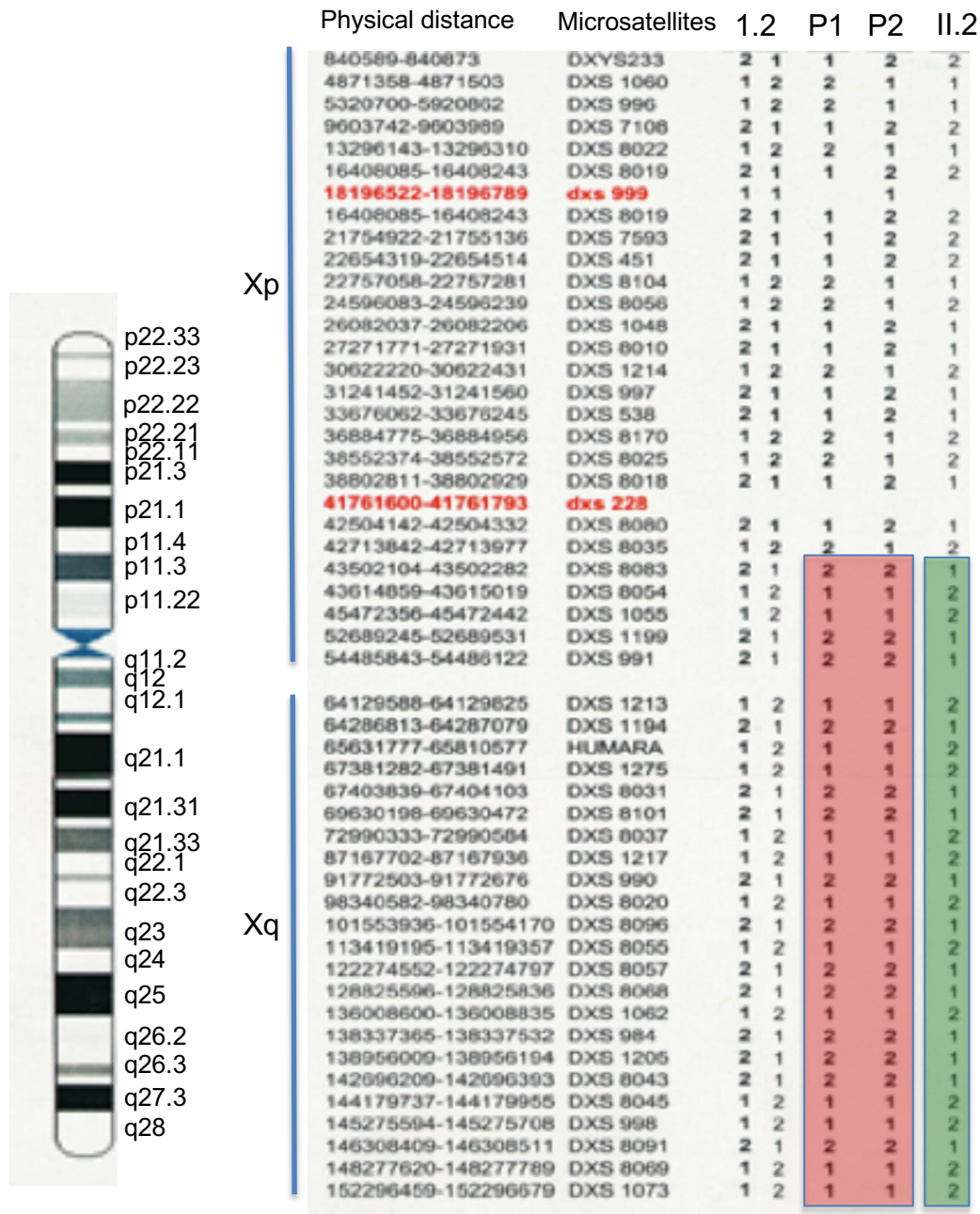
Bertrand Boisson^{1,2,3@*}, Yoshitaka Honda^{4*}, Masahiko Ajiro^{5,6#}, Jacinta Bustamante^{1,2,3,7#},
Matthieu Bendavid^{1#}, Andrew R. Gennery^{8#}, Yuri Kawasaki⁹, Jose Ichishima⁹, Mitsujiro Osawa⁹,
Hiroshi Nihira⁴, Takeshi Shiba⁴, Takayuki Tanaka⁴, Maya Chrabieh^{2,3}, Benedetta Bigio¹, Hong
Hur¹⁰, Yuval Itan¹, Yupu Liang¹⁰, Satoshi Okada¹¹, Kazushi Izawa⁴, Ryuta Nishikomori⁴, Osamu
Ohara^{12,13}, Toshio Heike^{4,14}, Laurent Abel^{1,2,3}, Anne Puel^{1,2,3}, Megumu K. Saito^{9\$},
Jean-Laurent Casanova^{1,2,3,15,16,\$,@}, Masatoshi Hagiwara^{5,6\$} and Takahiro Yasumi^{4,\$@}

Supplementary Fig. 1. X-inactivation pattern in the leukocyte subsets and fibroblasts of the European mother
 PMBCs were purified (subset) and genomic DNA was extracted from each cell population. As a control, the X-inactivation patterns in the blood cells of a healthy female control and of a woman with IP carrying the common IP *NEMO*^{*Δ4-10/WT*}¹³ are shown.



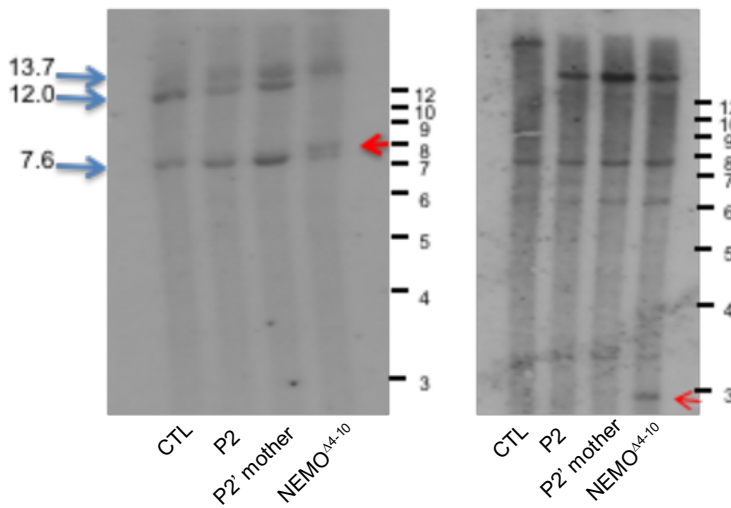
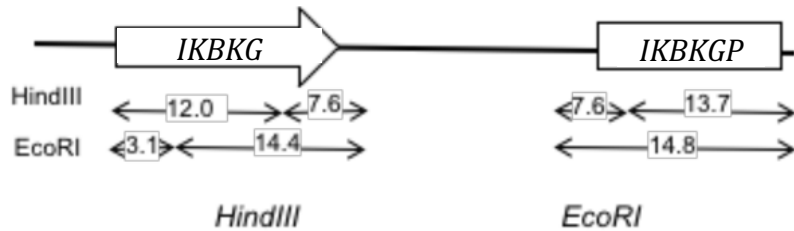
Supplementary Fig. 2. X-chromosome microsatellite analysis on DNA from the European mother, her two affected sons (P1, P2) and their healthy brother.

The red rectangle indicates the microsatellites common to P1 and P2 but different in A.II.3, the healthy brother (depicted in green), and inherited from the mother (A.I.2).



Supplementary Fig. 3. Analysis of the *IKBK*G and *IKBK*GP loci by Southern blotting.

We digested gDNA from one control, P2, his mother (P2' mother) and one male *IKBK*G-deficient patient carrying a deletion of exons 4-10 (*NEMO*^{Δ4-10/Y}) with *Hind*III or *Eco*RI. The resulting DNA fragments were separated by gel electrophoresis, transferred onto a membrane and hybridized with a radioactive *IKBK*G cDNA probe.

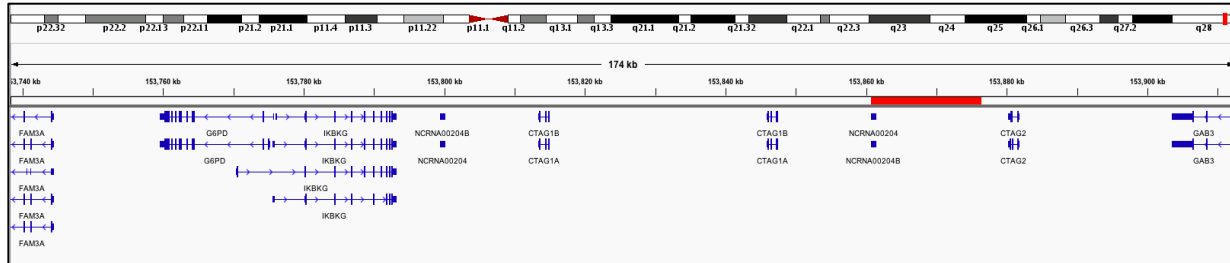


Supplementary Fig. 4. Visualization of WGS alignment at position X: 153,787,731.

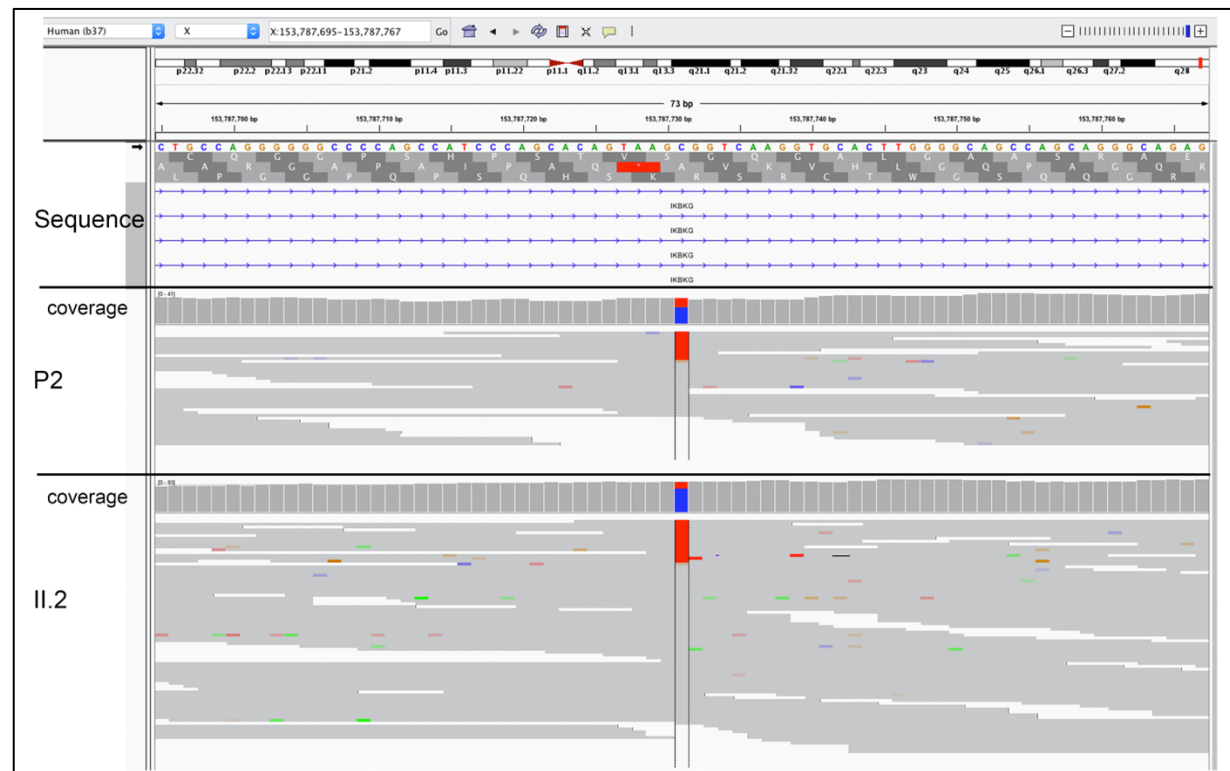
A. Chromosome masking strategy on the Hg19-B37 reference genome and sequences aligned at the point mutation. In red, the region masked during the alignment process to ensure that all sequences were associated with the *IKBK*G gene.

B. IGV snapshot of WGS analysis for P2 and C1. The reads carrying a T nucleotide at position 153,787,731 are shown in red, and those carrying a C in this position are shown in gray.

A.



B.



Supplementary Fig. 5. Summary of the new variants identified in our analysis and absent from the 1kG, ExAC and Esp6500 databases.

A. Variants found in the hemizygous state in males and or in the homozygous state in females. **B.** Variants found in the heterozygous state in males and/or females.

A

Male hemizygous	X		X	X	X	X		
Male heterozygous	X		X			X	X	
Female homozygous	X	X					X	
Female heterozygous	X	X	X	X			X	
Location	count	count	count	count	count	count	count	Total
downstream	33		18	4	7	4	1	67
indel-frameshift								0
intron	26	2	14	6	1	1	1	51
missense			1					1
splicing	1							1
stop-gained								0
synonymous								0
utr_3	3		1	2				6
Total	63	2	34	12	8	5	2	126

B

Male hemizygous				
Male heterozygous		X	X	
Female homozygous				
Female heterozygous	X	X		
Location	count	count	count	Total
downstream	77	36	27	140
indel-frameshift			1	1
intron	94	47	48	189
missense	7	7	7	21
splicing		1		1
stop-gained	1	1		2
synonymous	6	1	2	9
utr_3	9	8	3	20
Total	194	101	88	383

X : present in this category

Supplementary Fig. 6. 3'ss (splice acceptor) and 5'ss (splice donor) prediction by ESE finder and other software. Predicted splice acceptor and donor sites from 100 bp upstream to 100 bp downstream from the IVS4+866 mutation. Predictions were obtained with ESE Finder ver. 3.0 (http://krainer01.cshl.edu/cgi-bin/tools/ESE3/ese_finder.cgi?process=home)⁴⁴. Predicted sites above the standard threshold (6.632 for 3'ss and 6.670 for 5'ss) are indicated for the reference sequence (A) and the IVS4+866 C>T-sequence harboring intron 4 of *IKBK*G (B). Results obtained with other software (C). MT indicates IVS4+866 C>T. PE: pseudo-exon.

A. WT genomic *IKBK*G sequence (IVS4 from +767 to +967)

gggcagggagggtttctgtggttctcattcggctctgcttctgccctccagacagatggatcagctgccaggg
3'ss U2/human
Score 9.71
gggccccagccatcccagcacagtaagCgggtcaaggtgcacttggggcagccagcagggcagaggggagggg
5'ss U2/human
Score 7.35
agcttgaccagggtctctgatgggcagaggggaaccctgcaggggtgtgggggcagta

B. IVS4+866 C>T genomic *IKBK*G sequence (IVS4 from +767 to +967)

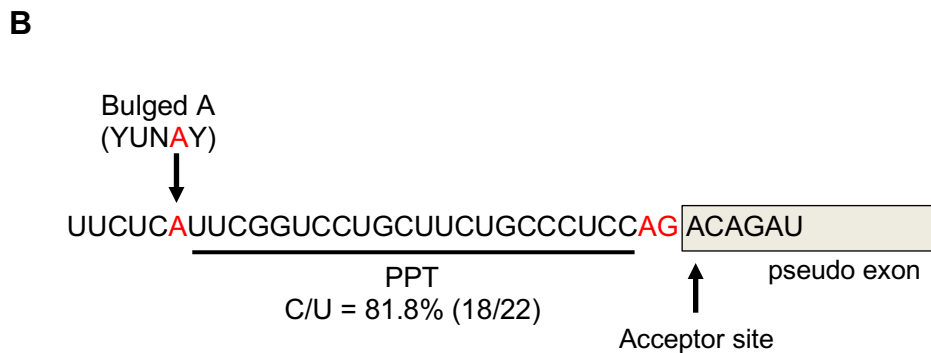
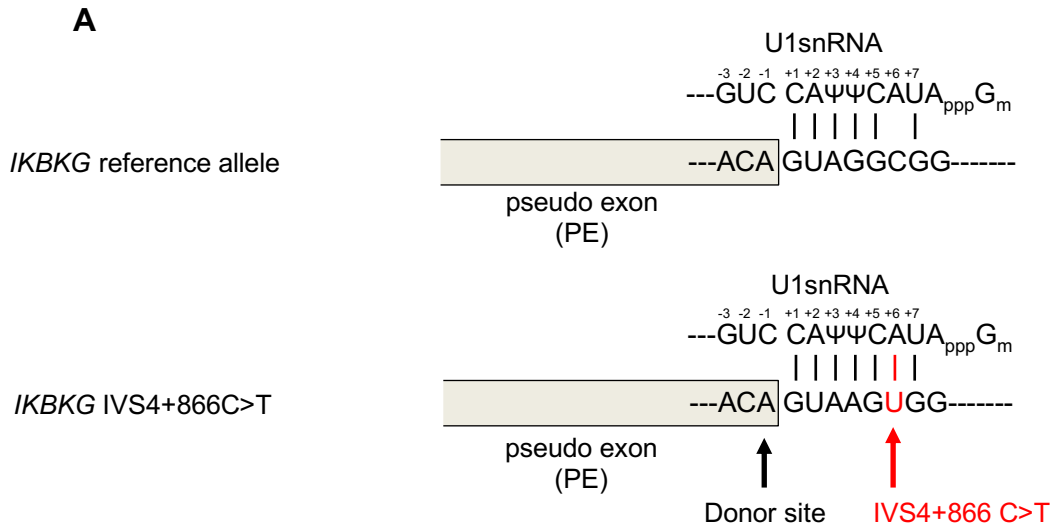
gggcagggagggtttctgtggttctcattcggctctgcttctgccctccagacagatggatcagctgccaggg
IVS4+866 C>T
3'ss U2/human
Score 9.71
gggccccagccatcccagcacagtaagTgggtcaaggtgcacttggggcagccagcagggcagaggggagggg
5'ss U2/human
Score 8.55
agcttgaccagggtctctgatgggcagaggggaaccctgcaggggtgtgggggcagta

C. Splicing prediction of IVS4+866 C>T

Software Web site		Acceptor Exon 4	Donor Exon 4	Acceptor Exon 5	Donor Exon 5	Acceptor PE	Donor PE	Pred. 44pb exon
NetGene 2 High:0.95, probably .50	WT	0	0.99	0.95	0	0.56	0.79	?
	MT	0	0.99	0.95	0	0.56	0.83	?
GenScan (MIT) none above the cut-off genes.mit.edu/GENSCAN.html	WT	45	109	94	81	95	72	Yes
	MT	45	109	94	81	95	98	Yes
SpliceView	WT	85	88	88	87	89	82	No
	MT	85	88	88	87	89	85	No
SplicePort (pos:true, neg: false) spliceport.cbc.umd.edu	WT	No	0.31	1.17	No	0.69	0.08	No
	MT	No	0.31	1.17	No	0.78	0.95	No
Alternative Splice Site Predictor	WT	No	13.0	8.0	9.3	9.1	9.0*	No
	MT	No	13.0	8.0	9.3	9.1	11.8	No
Human Splicing Finder www.umd.be/HSF3/	WT	90.6	92.1	88.7	86.5	91.0	81.5	
	MT	90.6	92.1	88.7	86.5	91.0	83.7	
RegRNA	WT	No	10.2	8.2	No	7.5	7.7	No
	MT	No	10.2	8.2	No	7.2	9.9	No
Fruitfly (cutoff: 0.40)	WT	0.90	0.98	0.97	0.97	0.88	0.95	No
	MT	0.90	0.98	0.97	0.97	0.88	0.96	No

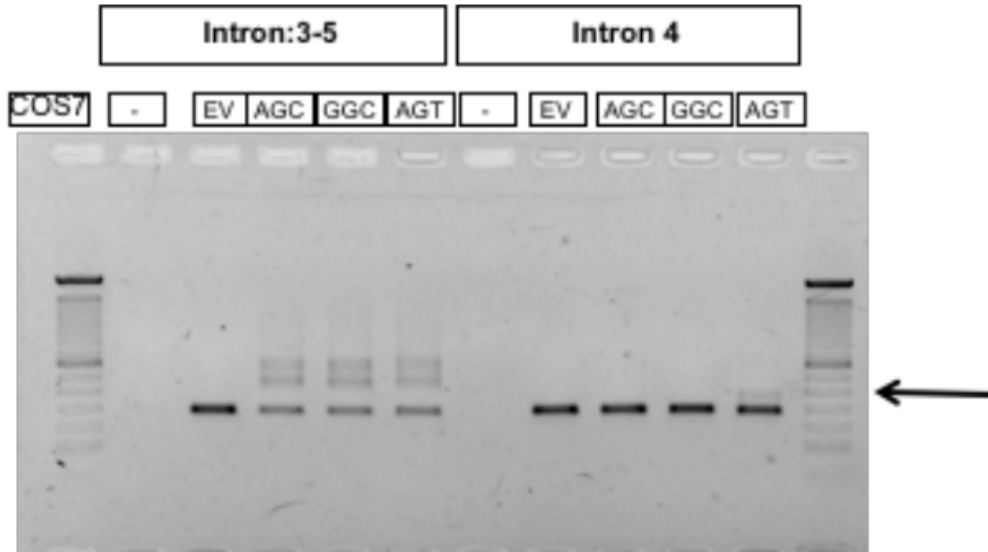
Supplementary Fig. 7. Schematic diagram of the 44 nt pseudo-exon

Base-pairing to U1 snRNA (A) and consensus motifs of a splice acceptor site, branch point (YUNAY: Y, pyrimidine; N, any base), and polypyrimidine tract (PPT) (B) are shown for the 44 nt pseudo-exon created by the IVS4+866 C>T mutation.

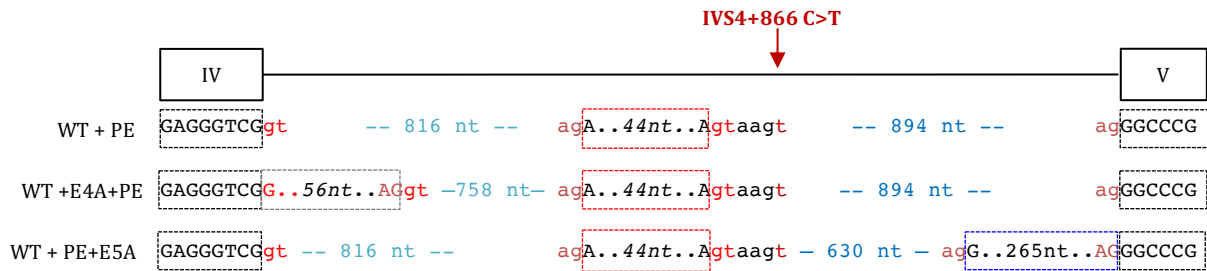


Supplementary Fig. 8. Exon trapping for the intronic *IKBK* region with and without the IVS4+866 C>T mutation
A. PCR amplification of the transcript after the transfection of COS7 cells with empty plasmid or with the genomic sequence between introns 3 and 5 or part of intron 4 only. **B.** Schematic view of the new transcripts due to the IVS4+866 C>T mutation, obtained by exon trapping. NT; nucleotide, PE; pseudo-exon, E4A; exon 4A, E5A; exon 5A. See Supplementary Fig. 9 for the details.

A

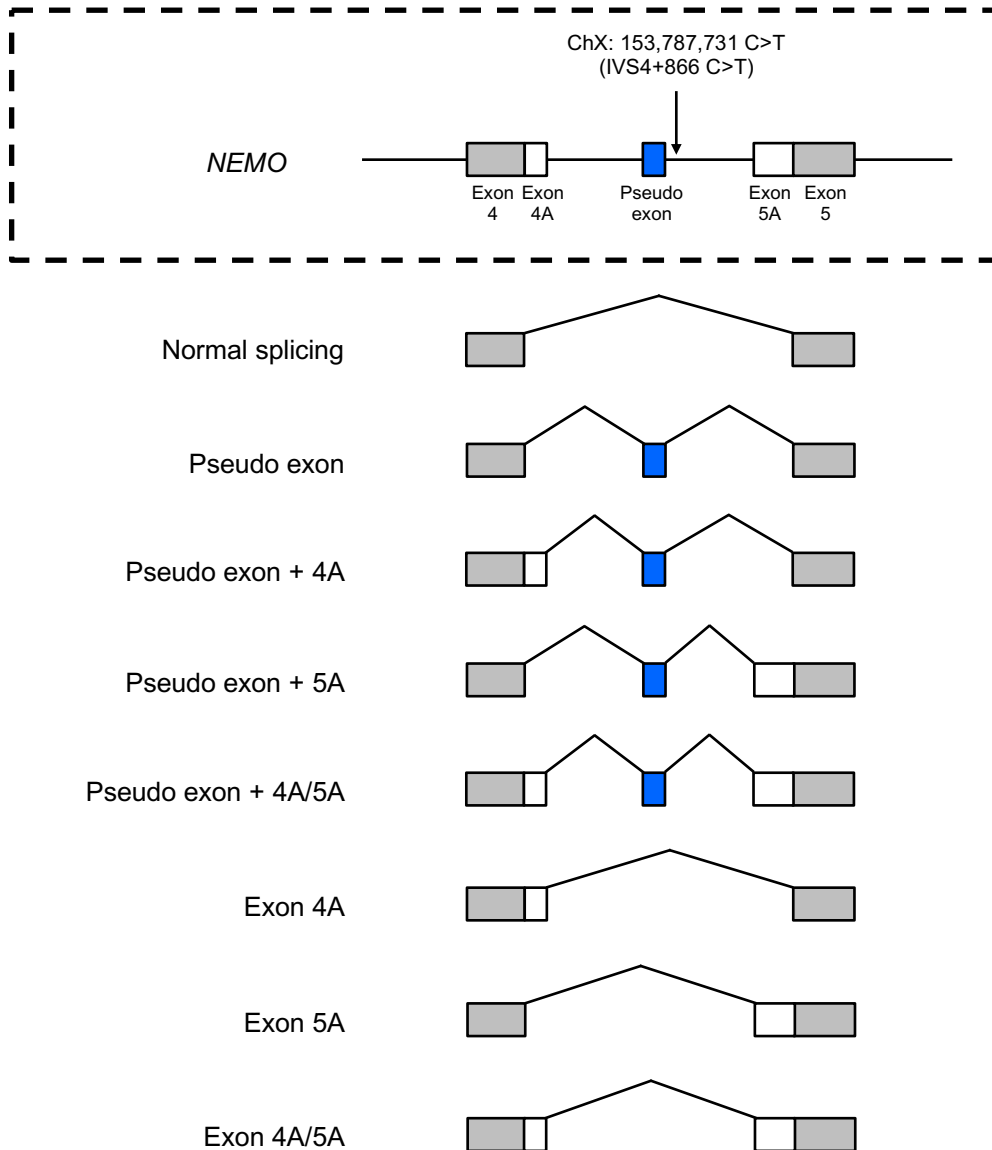


B



Supplementary Fig. 9. Diagram of the 44 nt pseudo-exon and alternative splicing products from *IKBK* exon 4 through exon 5

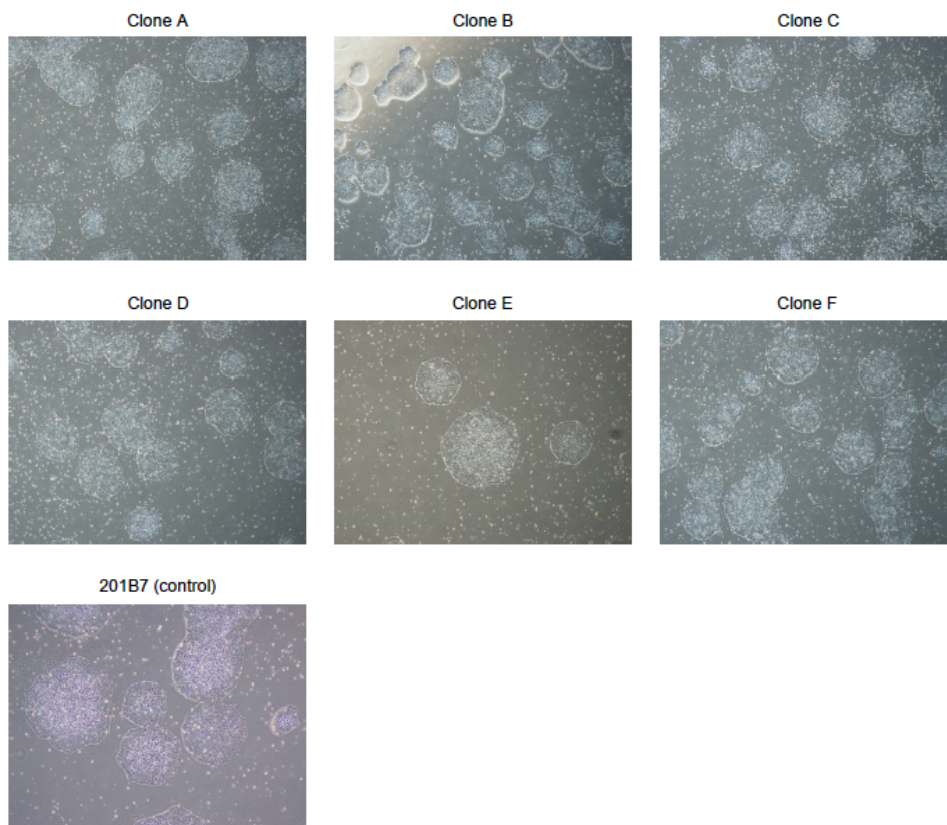
The pseudo-exon (closed box in blue), exon 4 with the alternative splice site (exon 4A), exon 5 with the alternative acceptor site (exon 5A), exons 4 and 5 are indicated for *IKBK*. Introns are indicated as a horizontal bar. Identified splice products, including normal splicing products, pseudo-exon, pseudo-exon + 4A, pseudo-exon + 5A, pseudo-exon + 4A/5A, exon 4A, exon 5A, and exon 4A/5A are shown below.



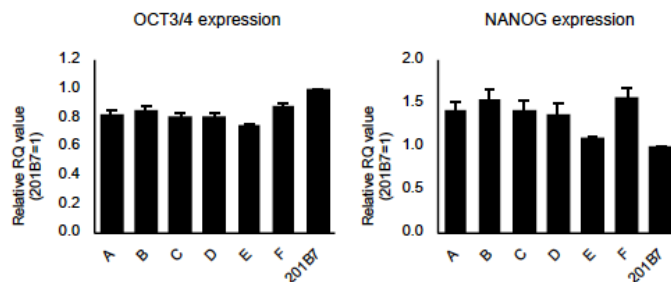
Supplementary Fig. 10. Basic characterization of iPSCs, iPSC-derived myeloid cells (iPSC-MLs), and iPSC-derived neural progenitor cells (iPSC-NPs).

A. Bright-field micrographs of iPSC morphologies. **B.** Expression of pluripotency-associated genes ($n=3$), bars indicate the minimum and maximum RQ values. Expression is shown relative to that of the 201B7 control clone. **C.** Quantification of the copy number of residual plasmids per cell. The copy numbers of the CAG promotor region and EBNA sequence were determined. Each clone was analyzed at passage 2. **D.** Bright-field micrographs with May-Giemsa staining for iPSC-ML clones (A, B, C, D, E, and F, and a control from a healthy individual (201B7)). **E.** Bright-field micrograph of P3 iPSC-derived neurospheres, which were used as neural progenitor cells (iPSC-NP) in this study. Scale bar, 500 μm . **F.** Fluorescence immunostaining of a P3 iPSC-NP neurosphere (clones A and F), for Pax6 (red) and Nestin (green), with 4', 6-diamidino-2-phenylindole (DAPI) staining of the nucleus (blue). Scale bar, 200 μm .

A



B

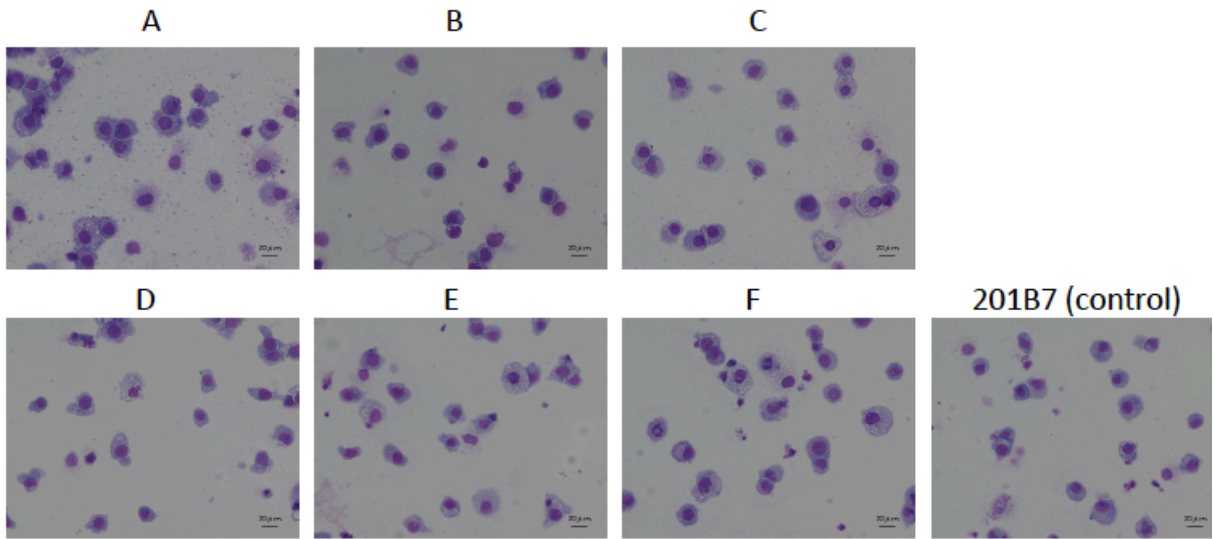


C

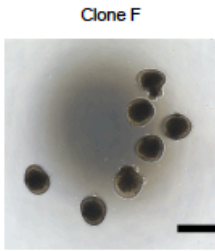
Clones	CAG	EBNA
A	0.025	0.036
B	0.157	0.185
C	0.098	0.122
D	0.074	0.086
E	0.080	0.107
F	0.118	0.141

(copies/ cell)

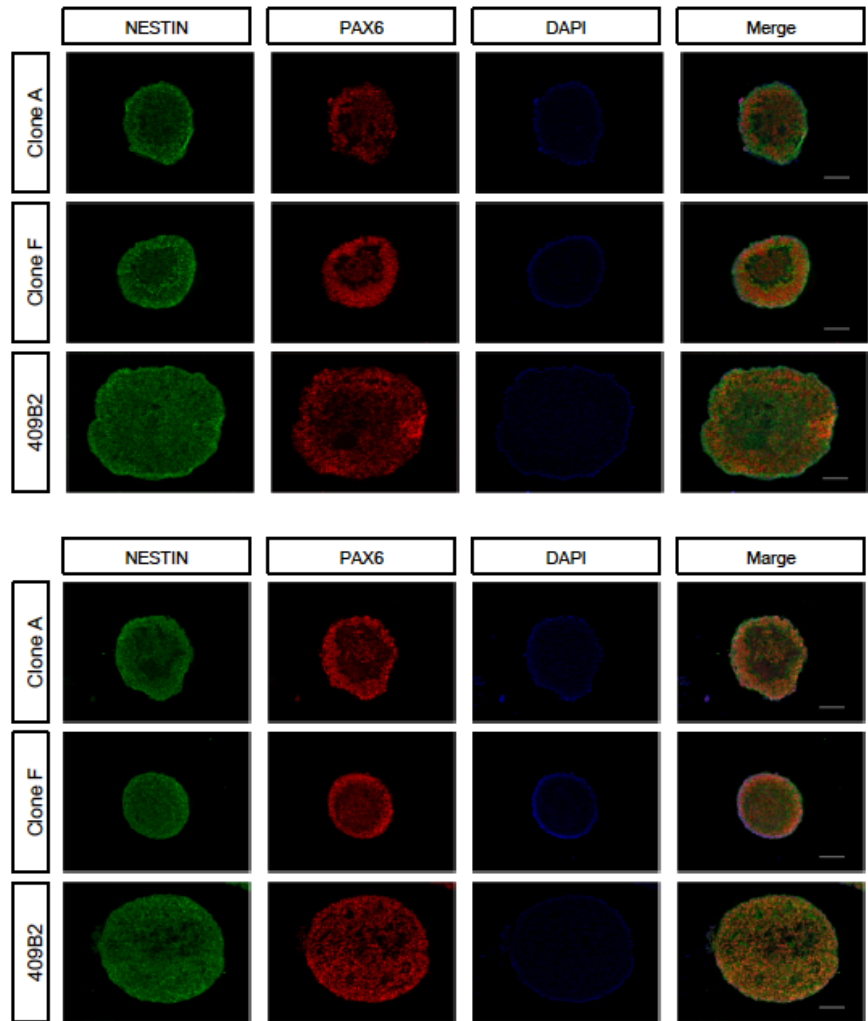
D



E

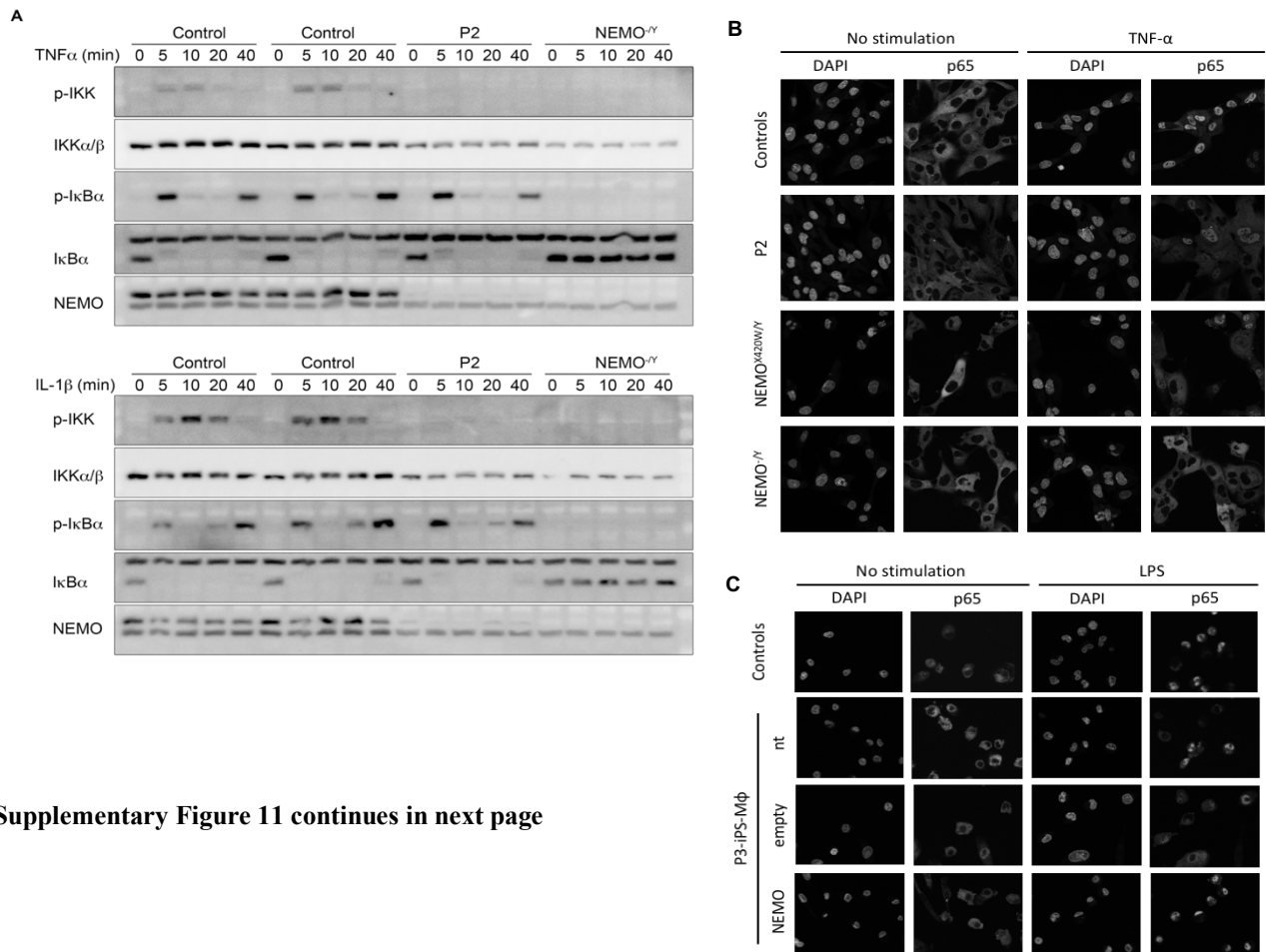


F



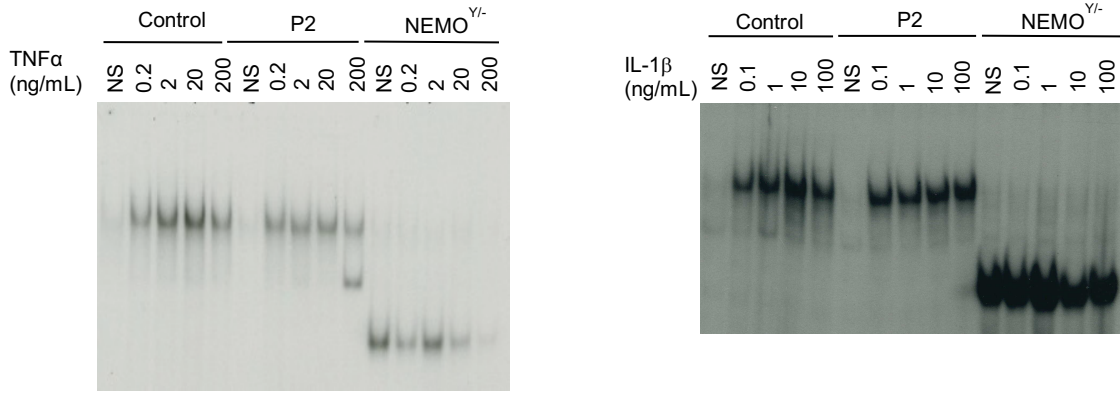
Supplementary Fig. 11. NEMO insufficiency impairs NF- κ B activation in the cells of the patients

A. Impaired NF- κ B activation in response to IL-1 β . Time-course for IL-1 β - and TNF α -stimulated SV40-immortalized fibroblasts, showing impaired IKK α/β phosphorylation but no impairment of I κ B α degradation in P2 relative to a control. **B and C.** Representative immunofluorescence images used for the quantification of p65 translocation in the nucleus after fixation and staining with anti-p65 and DAPI. Fibroblast (B) and iPSC (C) cells were stimulated for 60 minutes with LPS. **D.** Nuclear protein extracts from the SV-40-immortalized fibroblasts of a control, P2 and a male *NEMO*-deficient patient, with and without stimulation for 20 minutes with various doses of TNF α or IL-1 β , were incubated with a ³²P-radiolabeled specific NF- κ B-binding probe. **E.** Impaired IL-6 production in response to TNF α , TNF β , IL-1 β , poly(I:C), IL-17 and PMA in P2' SV-40-immortalized fibroblasts and two reported *NEMO*-deficient patients (*NEMO*^{X420W/Y} and *NEMO*^{A4-10/Y}). Two different SV-40-immortalized fibroblasts controls were used. N=3 or 4. **F.** Exogenous NEMO expression in the P3 iPSCs was achieved by stable transfection of the cells with an expression vector encoding the full-length NEMO. The resulting iPSCs were then differentiated into iPSC-M ϕ for further analysis. of the successful rescue of full-length NEMO expression was confirmed by western blotting. β -actin served as a loading control (ACTIN). **G.** Impaired NF- κ B p65 nuclear translocation in P3 iPSC-M ϕ . NF- κ B p65 nuclear translocation induced by TNF- α stimulation was rescued by re-expressing WT NEMO (P3+NEMO) to the levels slightly short of control cells. Data is shown as mean \pm SD of cells from more than four random fields in each well and the number of cells analyzed in each condition are shown in parentheses. Representative result of three independent experiments is shown. **, $p < 0.001$, *, $p < 0.05$ by one-way ANOVA followed by Turkey's test for multiple comparisons. ns, not significant. **H.** Impaired TNF α production in P3 PBMCs. LPS dose-responsive TNF α production in controls and P3 PBMCs in the presence of 5,000 U/mL IFN γ . TNF α production was measured after 24 h of stimulation. **I.** Impaired production of TNF α in P3 monocytes. PBMCs from P3 or a control were stimulated with LPS in the presence of monensin to block the protein secretion. Four hours later, cells were stained for CD14 and TNF α and analyzed by flow cytometry.

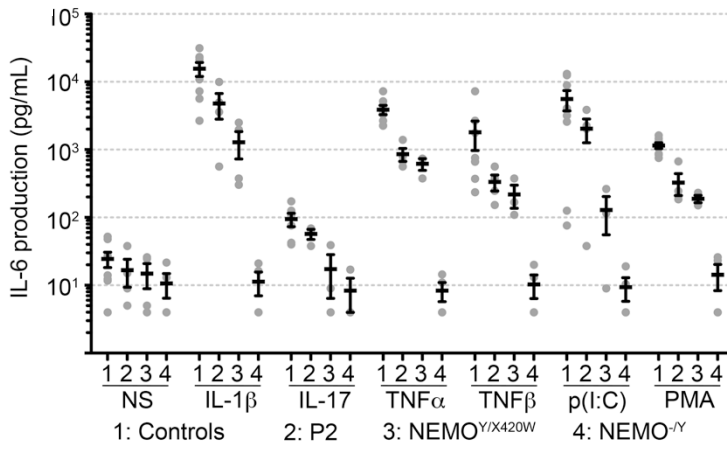


Supplementary Figure 11 continues in next page

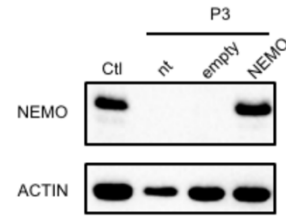
D



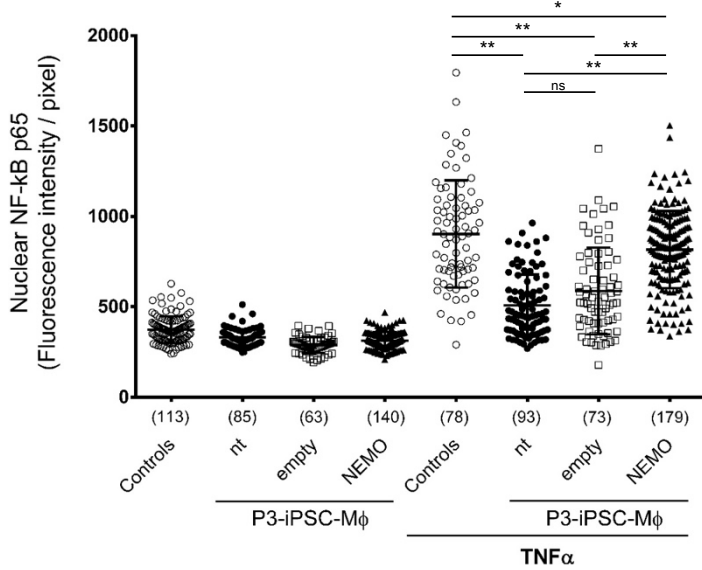
E



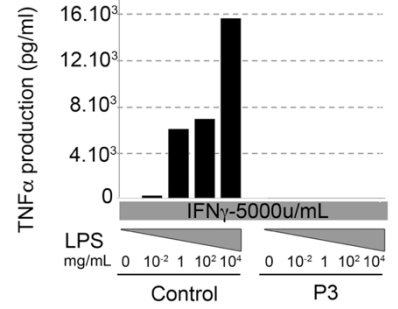
F



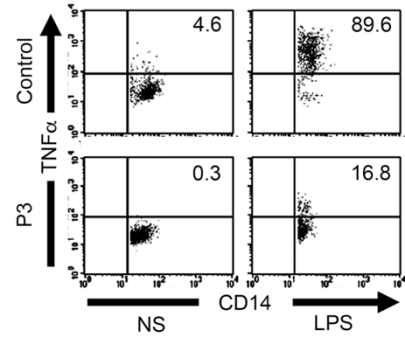
G



H

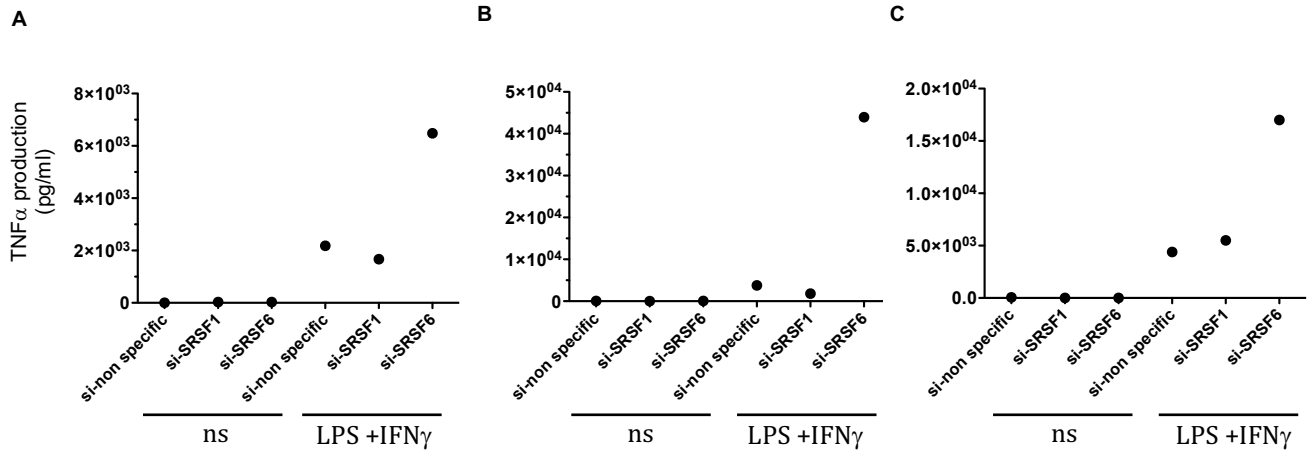


I



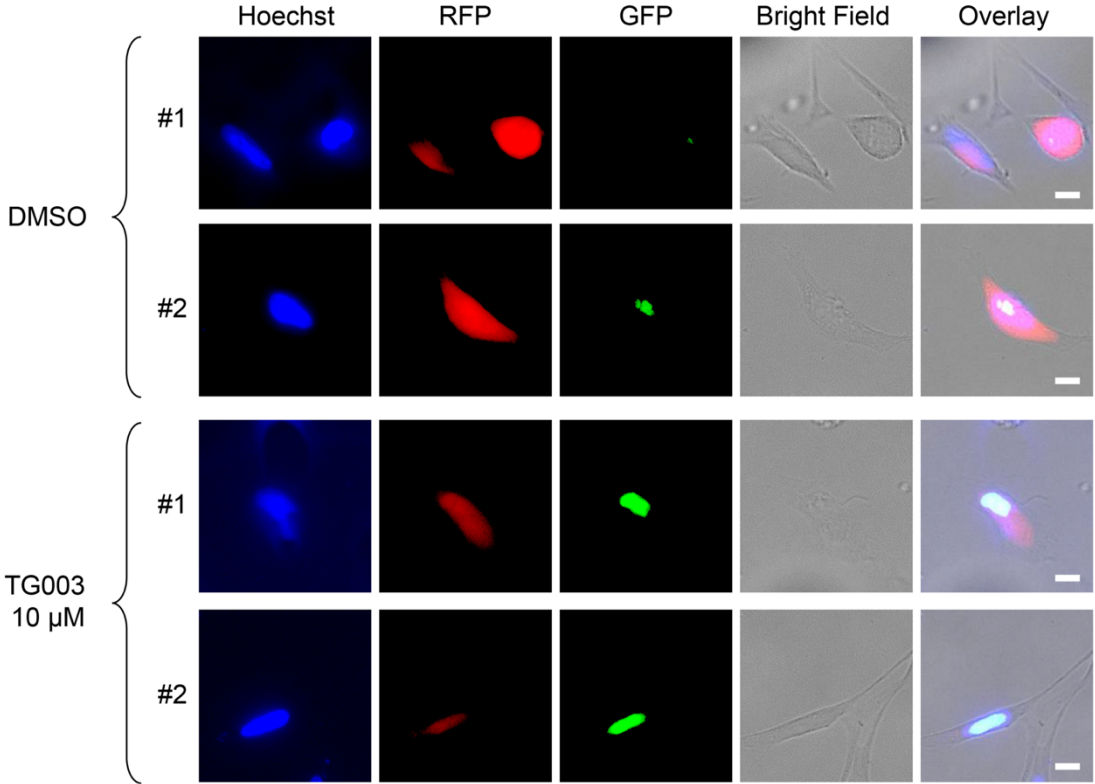
Supplementary Fig. 12. TNF α production from P3 iPSC-M ϕ clones upon stimulation with LPS and IFN γ

Three independent P3 iPSC (used to depict the figure 7E) clones were differentiated into iPSC-M ϕ , transfected with siRNAs (si-SRSF1, si-SRSF6, or non-targeting siRNA control) and stimulated with LPS and IFN γ for the assessment of TNF α production. (A) Clone 1, (B) clone 2, (C) clone 3.



Supplementary Figure 13. Magnified fluorescence image for *IKBK*G SPREADD reporter-transfected cells.

HeLa cells, transfected with *IKBK*G SPREADD reporter, were treated with 0.1% DMSO or 10 μ M TG003. Nuclei were counterstained with Hoechst33342. Fluorescence images were overlaid with phase contrast/bright field images. Scale bar, 10 μ m.



Supplementary tables

Supplementary Table 1. Immunological profile of the P2

Supplementary Table 2. Variant identified in our analysis of the 1,000 Genomes project data from 2,500 individuals from five different ethnic groups

Supplementary Table 3. Rare and common coding variants at the *IKBKG* locus based on this study, and the 1000 Genomes project, ExAC and ESP6500 databases.

Supplementary Table 4. Summary of *IKBKG* sequencing analysis

Supplementary methods

Rescue of recurrent deep intronic mutation underlying cell type-dependent quantitative NEMO deficiency.

Bertrand Boisson^{1,2,3@*}, Yoshitaka Honda^{4*}, Masahiko Ajiro^{5,6#}, Jacinta Bustamante^{1,2,3,7#},
Matthieu Bendavid^{1#}, Andrew R. Gennery^{8#}, Yuri Kawasaki⁹, Jose Ichishima⁹, Mitsujiro Osawa⁹,
Hiroshi Nihira⁴, Takeshi Shiba⁴, Takayuki Tanaka⁴, Maya Chrabieh^{2,3}, Benedetta Bigio¹, Hong
Hur¹⁰, Yuval Itan¹, Yupu Liang¹⁰, Satoshi Okada¹¹, Kazushi Izawa⁴, Ryuta Nishikomori⁴, Osamu
Ohara^{12,13}, Toshio Heike^{4,14}, Laurent Abel^{1,2,3}, Anne Puel^{1,2,3}, Megumu K. Saito^{9§},
Jean-Laurent Casanova^{1,2,3,15,16,\$,@}, Masatoshi Hagiwara^{5,6§} and Takahiro Yasumi^{4,\$@}

Methods

Genome-wide analysis

Genome-wide human SNP array: Genomic DNA was isolated from the peripheral blood of the P1 and P2 patients, a healthy sister and their mother, by the phenol/chloroform method. The GeneChip Genome-Wide Human SNP Array 6.0 (Affymetrix, Santa Clara, CA) oligonucleotide-based array was used according to the manufacturer's instructions. The data were analyzed and displayed with Affymetrix Genotyping Console 4.0 software and the Affymetrix Genotyping Console Browser.

WES: Genomic DNA (3 µg) extracted from the peripheral blood cells of the patients was sheared with a Covaris S2 Ultrasonicator (Covaris). An adapter-ligated library was prepared with the Paired-End Sample Prep kit V1 (Illumina). Exome capture was performed with the SureSelect Human V4+UTR kit (Agilent Technologies). Paired-end sequencing was performed on a HiSeq 2500, generating 100-base reads.

WGS: WGS was performed with PCR-Free prep on a HiSeq 2500 machine.

Sequence alignment, variant calling and annotation: The sequences were aligned with the human genome reference sequence (hg19 build) after manual editing to replace all the nucleotides between chrX:153,860,736-153,876,549 with “N”, using BWA aligner(1). Downstream processing was carried out with the Genome analysis toolkit (GATK)(2), SAMtools(3) and Picard Tools (<http://broadinstitute.github.io/picard/>). Substitution calls were made with a GATK UnifiedGenotyper, whereas indel calls were made with a GATK IndelGenotyperV2. All calls with a read coverage $\leq 2x$ and a Phred-scaled SNP quality of ≤ 20 were filtered out. All the variants were annotated with the GATK Genomic Annotator.

RNA-Seq:

The fastq files were first subjected to quality control, with FastQC v0.11.15 (<https://www.bioinformatics.babraham.ac.uk/projects/fastqc/>), using the default parameters. Cutadapt v1.9.1(4) was used to trim the sequences to remove low-quality bases and TruSeq adapters (--times=2 --quality-base=33 --quality-cutoff=5 --format=fastq --minimum-length=25 -a AAAAAAAAAAAAAA TTTTTTTTTTTTTT -a AGATCGGAAGAG -a CTCTTCCGATCT). Trimmed fastq files were aligned to the masked human genome (pseudo-gene *IKBKGP* was masked from GRCH37 with bedtools) with the STAR v2.4.2a(5) aligner, using default parameters. The alignment results were then evaluated with Qualimap v.2.2(6), to ensure that all the samples had a consistent coverage, alignment rate, and no obvious 5' or 3' bias. Aligned reads were then visualized with Integrative Genome Viewer from Broad.

WGS reanalysis: 1,000 Genomes download sequence

We downloaded all reads mapping between 153,700,000 and 154,000,000 on chromosome X from the 1,000 Genomes Phase 3 BAM database with Samtools (e.g. `./samtools view -h ftp://ftp.1000genomes.ebi.ac.uk/vol1/ftp/phase3/data/HG00096/alignment/HG00096.mapped.ILLUMINA.bwa.GBR.low_coverage.20120522.bam X:153700000-154000000`). This dataset corresponds to 2,534 individuals of different origins. Paired sequences were extracted with the `cat` command (`cat NA21144.mapped.ILLUMINA.bwa.GIH.low_coverage.20130415.fastq | grep '^@.* /1$' -A 3 | sed '/^--$/d'`). Sequences were realigned by applying the above pipeline to the HG19 (B37) genome after masking the 153860736~153876549 region. Calls were made according to the following parameters: `MQ>50`, `reads>4`, `quality>30`, and at least 100 individuals were called at this position. We used the *IKBKG* locus as defined in ENSEMBL GRCh37.p13 (X:153,769,414-153,796,782).

Web resources

NCBI Aceview: <https://www.ncbi.nlm.nih.gov/iebr/research/acembly/av.cgi?db=human&term=IKBKG&submit=Go>

Bravo: <https://bravo.sph.umich.edu>

gnomAD: gnomad.broadinstitute.org/

ESE finder: (ver. 3.0) <http://krainer01.cshl.edu/cgi-bin/tools/ESE3/esefinder.cgi?process=home>

Cell lines, immortalization and complementation

Fibroblasts from the patients and controls were immortalized by transfection with a plasmid containing the simian virus 40 large T antigen gene. Transformed cell lines were grown in DMEM (GIBCO®#10566) supplemented with 10% fetal calf serum (GIBCO®#16000). The NEMO^{A4-10/WT} fibroblast cell line used in experiments was kindly provided by Dr A. Smahi(7) (Imagine Insitute, Paris, France). HeLa was obtained from Riken BRC.

Establishment and maintenance of iPSCs

Induced pluripotent stem cells (iPSCs) were generated from blood cells, as previously described(8, 9). Briefly, blood cells were isolated from peripheral blood with a BD Vacutainer (BD Biosciences, San Jose, Calif), in accordance with the manufacturer's instructions. The PBMCs were cultured in StemSpan-ACF medium (STEMCELL Technologies, Vancouver, British Columbia, Canada) supplemented with stem cell factor (SCF; 100 ng/mL), thyroperoxidase (TPO; 100 ng/mL), Flt ligand (100 ng/mL), IL-6 (50 ng/mL), and IL-3 (10 ng/mL) for five days before transfection. SCF, TPO, Flt ligand, IL-6, and IL-3 were purchased from R&D Systems (Minneapolis, Minn). Episomal plasmids (3 µg) mixed with pCE-hOCT3/4, pCE-hSK, pCE-hUL, pCE-mp53DD, and pCXBEBNA1 were used to transfect 1 to 2×10⁶ cultured PBMCs in a Nucleofector 2b device, with the Amaxa Human CD34 cell Nucleofector kit. The electroporated cells were plated on tissue-culture plates coated with the Laminin511-E8 fragment iMatrix-511 (Nippi, Tokyo, Japan) and containing StemSpan-ACF medium supplemented with the cytokines listed above. The culture medium was gradually replaced with StemFit AK03 medium (Ajinomoto, Tokyo, Japan). Two to three weeks after transduction, individual colonies were isolated and expanded. The iPSCs were cultured on LN511E8-coated tissue-culture plates with StemFit AK03 medium at 37°C under an atmosphere containing 5% CO₂ and 21% O₂ and were passaged by dissociation into single cells with TrypLE Select (Life Technologies, Gaithersburg, Md), as previously described. The human iPSC line 201B7E1 was kindly provided by Dr Shinya Yamanaka (Kyoto University, Kyoto, Japan) and was used as a control.

Characterization of established iPSCs

Chromosomal G-banding analyses were performed at the Nihon Gene Research Laboratory (Miyagi, Japan). For the teratoma formation assay, approximately 2×10^6 cells were injected subcutaneously into the dorsal flank of immunocompromised NOD/scid/ccnull mice (Central Institute for Experimental Animals, Kawasaki, Japan). Masses were excised 9 to 14 weeks after injection and fixed with 4% paraformaldehyde in PBS. Paraffin-embedded tissues were sliced and stained with hematoxylin and eosin. Slides were examined with a BIOREVO BZ-9000 microscope (Keyence, Osaka, Japan). A PlanApo 103/0.45 objective (Nikon, Tokyo, Japan) and the BZ-II Viewer software program (Keyence) were used for image acquisition.

Generation of NEMO-reconstituted iPSCs

Piggybac plasmids encoding wild-type *IKBKG* and blasticidin resistance (5 μ g) and transposase-encoding plasmids (5 μ g) were introduced into 1×10^6 patient-derived iPSCs with a NEPA21 electroporator (Nepa Gene, Japan). Three to four days later, blasticidin (5 μ g/mL; Wako, Japan) was added to the medium for the selection of NEMO-reconstituted cells. NEMO-reconstituted iPSC-MLs were established from these reconstituted cells as described below.

Generation of iPSC-MLs

iPSC-derived myeloid cells (iPSC-MLs) were established as previously described(10). In brief, floating hematopoietic cells differentiated into the monocytic lineage from iPSCs were collected on days 15 to 18. Cells were transfected with the lentiviral constructs encoding BMI1, cMYC, and MDM2 in the CSII-EF-RfA vector kindly provided by Drs Satoru Senju (Kumamoto University, Kumamoto, Japan) and Hiroyuki Miyoshi (RIKEN Bio Resource Center, Tsukuba, Japan), and cultured in StemPro-34 serum-free medium containing 2 mmol/L L-glutamine in the presence of

M-CSF (50 ng/mL) and GM-CSF (50 ng/mL). For macrophage differentiation, iPSCs were cultured in RPMI-1640 medium (Sigma-Aldrich) supplemented with 20% FBS and M-CSF (100 ng/mL) for 6 to 7 days. We then released adherent macrophages by Accumax (Innovative Cell Technologies, San Diego, Calif) treatment and collected the cells for subsequent experiments. For cytokine secretion assays, we stimulated 5×10^4 cells with LPS (1 $\mu\text{g/mL}$) and IFN γ (5000 U/mL) for 4 hours. Where indicated, cells were treated with TG003 for 24 hours before stimulation.

Generation of iPSC-derived neuronal precursor cells

iPSCs were differentiated into neuronal precursor cells (iPSC-NPs) the serum-free floating culture of embryoid body-like aggregated with quick reaggregation (SFEBq) method, as previously described(11).

Full-length amplification of the *IKBKG* and *IKBKGP* loci from gDNA

We amplified the 10 kb of *IKBKG* and pseudo-*IKBKG* (*IKBKGP*), using the Clone Amp Hifi DNA polymerase. The PCR mixture (total volume 25 μL) contained 12.5 μL buffer, 0.5 μL of each primer (10 μM stock solution) and 50 to 100 ng DNA. PCR was performed in a Perkin 2500 machine with the following program: 98°C for 2 min, 38 cycles of denaturation at 98°C for 10 s, annealing at 58°C for 15 s and elongation at 72°C for 90 s, with a final elongation at 72°C for 5 min.

The following primers were used: forward primer NEMO_F2: 5'-agcaggcaatagttagttggtgagg ; F2P: 5'-caagaagatcgcttggggtcg and reverse primer NEMO_R8:5'-acgcacgactaatgcacaagg and NEMO_R3: 5'-ttccctctgcccacagag

Northern blot

Denatured RNA (1 µg) was subjected to electrophoresis in an agarose-formaldehyde (1% agarose, 2.2 M formaldehyde) gel in MOPS buffer. The RNA bands obtained were transferred onto Hybond N+ (Amersham) nitrocellulose membranes by passive transfer in 2xSSC. RNA was immobilized on membrane the membrane with a UV-crosslinker and by heating at 80°C for 2 hours. The membrane was incubated with hybridization buffer (10% dextran sulfate, 5x SSC, 6 ml formamide, 2x Denhardt's solution, 0.1% SDS, 25 mM sodium phosphate, pH 7.6) containing 100 µg/mL nonspecific DNA (salmon sperm DNA) and then with P³²-radiolabeled *IKBKG* cDNA or with an actin cDNA probe. Membranes were washed in SSC/SDS buffer (0.1x, 0.1% final concentration). Membranes were then placed against X-ray film (Kodak).

Quantitative PCR

IKBKG and *GAPDH* expression levels were quantified with the Hs00415849_m1 (Thermo Fisher) and 4310884E (Applied Biosystems) probes, on cDNA, with the 7500 Fast_real Time PCR system (Applied Biosystems).

Topo cloning and exon trapping

Total RNA was extracted from SV-40 fibroblasts with a Qiagen kit. Where indicated, poly-A mRNA was isolated with an Oligotex Direct mRNA Mini Kit. The RNA was reverse-transcribed (Superscript III first-strand synthesis, Invitrogen), and the resulting cDNA was amplified by PCR. The PCR products were then purified with a DNA cleanup kit (Qiaquick PCR purification, Qiagen) and inserted into the pCRTM4-TOPO[®] vector according to the kit manufacturer's procedure. Exon trapping was performed by amplifying 1,728 bp of controls and patients with the

5'CCGctcgagCGGAGACCCCTTCCAGGG and 5'-
AAATATgcgggccgcAGCAGACTCAGGGAGGACG primers from the xx region of control and patient gDNA. The amplicons were inserted into the pSLP3 plasmid between the *XhoI* and *NotI* restriction sites (Gibco BRL). The plasmids were subjected to Sanger sequencing and were then used to transfect COS-7 cells. Total RNA was isolated 24 hours after transfection and reverse-transcribed (Superscript-III, Invitrogen). Two specific exonic primers (SD6, SA2) were used for amplification, and the amplicons were inserted into a TOPO-vector, which was used to transform DH10B cells. Plasmids from around 100 clones were purified and subjected to Sanger sequencing for each construct.

siRNA

iPSC-M ϕ were transfected with the indicated siRNAs in the presence of Lipofectamine RNAi-Max (Invitrogen), on day 3 of induction. On day 6, cells were harvested and stimulated with LPS (1 μ g/mL) and IFN γ (5,000 U/mL) for 4 hours, and their TNF α secretion was analyzed. The following siRNAs were used in this study: Silencer Select Negative Control siRNA (4390843, Thermo Fisher Scientific) for the control siRNA, s12725 (Thermo Fisher Scientific) for SRSF1-specific siRNA, and s12741 (Thermo Fisher Scientific) for SRSF6-specific siRNA.

RNA pull-down assay

The soluble fraction of HeLa cell lysate was prepared in lysis buffer (10 mM Tris-HCl (pH 7.4), 150 mM NaCl, 1 mM EDTA, 1% Triton X-100, 0.1% SDS, 0.25% sodium deoxycholate, and 10% glycerol, with a cocktail of protease (Nacalai Tesque) and phosphatase (Sigma Aldrich) inhibitors), and incubated with 5'-biotin, 3'-dTdT-attached RNAs (5'-pseudo exon (oAM308), 5'-

biotin-acagauggaucagcugccaggggggc-dTdT; 3'-pseudo exon (oAM309), 5'-biotin-aggggggccccagccauccagcaca-dTdT; WT (oAM310), 5'-biotin-cagccauccagcacaguaggcggtc-dTdT; M1 (oAM311) 5'-biotin-cagccauccagcacaguaagUggtc-dTdT) for 16 h, with rotation, at 4°C. The proteins were then washed three times with TBS and eluted in Laemmli buffer. The eluted proteins were analyzed by western blotting with following antibodies: anti-SR protein mouse monoclonal antibody (Thermo Fisher Scientific, #33-9400, clone 1H4G7)) for phosphorylated SR proteins, anti-SNRPB mouse monoclonal antibody (Thermo Fisher Scientific, #MA5-13449, clone Y12) for SmB/B', anti-U1-A rabbit monoclonal antibody (abcam, #ab166890, clone EPR10632), anti-SNRPC rabbit monoclonal antibody for U1-C (abcam, #ab192028, EPR16034), and anti-U1-70k (Millipore, #05-1588, clone 9C4.1) mouse monoclonal antibody.

SPREADD reporter assay

A splicing reporter assay for disease genes with dual color (SPREADD) reporter vector for *IKBK*G exon 4 to exon 5 with the IVS4+866C>T mutation (pAM90) was designed and constructed as previously described(12). In this system, the exon 4⁵ splicing product provides an open reading frame (ORF) for green fluorescent protein (GFP), whereas the 44 nt pseudo-exon inclusion product provides an ORF for red fluorescent protein (RFP), translated following glutathione-S-transferase (GST) treatment. Seventy-three nucleotides of exon 4, 53 nucleotides of exon 5, and the entire IVS4 were included in the reporter. We used 0.2x10⁶ HeLa cells to seed each well of a six-well plate, and the cells were then transfected with the pAM90 reporter plasmid in the presence of Lipofectamine 2000 (Thermo Fisher Scientific). Five hours after transfection, the cells were treated with various chemical compounds for 24 h, and fixed by incubation with 4% PFA for 15

min. Fluorescence images were obtained with a BZ-X710 microscope (Keyence, Osaka, Japan) and quantified with Hybrid cell count BZ-H3C software (keyence).

Immunocytochemistry

iPSC-M ϕ or fibroblasts were used to seed multi-well glass-bottomed dishes (Matsunami). After 16 hours, the cells were stimulated with LPS (Invitrogen, 100 ng/mL) or TNF α (R&D, 10 ng/mL) for 60 minutes. They were then fixed with 4% paraformaldehyde in PBS for 30 minutes. Permeabilization and blocking were performed with blocking buffer (Blocking One (Nacalai Tesque) with 0.1% Tween 20 (Wako)) for 30 minutes. Samples were incubated with anti-NF- κ B p65 rabbit mAb (1:400; Cell Signaling Technologies, #4764, clone C22B4, Danvers, Mass) in blocking buffer overnight at 48°C and then with Alexa Fluor 488 goat anti-mouse IgG (1:1000; Cell Signaling Technologies) for 30 minutes. The nuclei were stained with DAPI (1:100) in PBS. The cells were visualized with a FluoVIEW10i confocal microscope (Olympus, Tokyo, Japan) and analyzed with ImageJ software (National Institutes of Health, Bethesda, Md).

Electrophoretic mobility shift assay (EMSA)

Nuclear extracts were obtained as described by Ramaswami and Hayden (13). In brief, cells were suspended in relaxation buffer (10 mM HEPES, pH 7.5, 10 mM KCl, 3 mM NaCl, 3 mM MgCl₂, 1 mM EDTA, 1 mM EGTA) and incubated for 20 min before lysis in 0.5% Igepal CA-630 (NP-40; Sigma, St. Louis, MO, USA). The lysed cells were centrifuged (1,000 x g, 5 min) and the supernatant was removed. The nuclei in the pellet were then lysed in nuclear extract buffer (20 mM HEPES, pH 7.9, 0.4 M NaCl, 0.1 mM EDTA) for 15 seconds and centrifuged (14,000 x g, 10 min). EMSA was performed by incubating 10 μ g of nuclear extract with a ³²P-labeled double-

stranded NF- κ B-specific oligonucleotide probe (5'-GATCATGGGGAATCCCCA and 5'-GATCTGGGGATTCCCCAT).

Cell lysis, immunoprecipitation and immunoblotting

Cells were lysed in a lysis buffer containing 30 mM Tris-HCl pH 7.5, 120 mM NaCl, 2 mM KCl, 1% Triton X-100 and 2 mM EDTA supplemented with protease inhibitor cocktail (Complete, Roche) and phosphatase inhibitor cocktail (PhoStop, Roche). Laemmli buffer supplemented with DTT was added to clear the supernatants. Samples were separated by SDS-PAGE and the bands obtained were transferred to a PVDF membrane. The membrane was blocked by incubation in TBS supplemented with 0.1% Tween 20 and 5% bovine serum albumin (fraction V) and incubated with the primary antibody, followed by the appropriate horseradish peroxidase-conjugated secondary antibody.

Activation by TLR agonists and cytokines

Where indicated, the cells were treated with human TNF α (R&D Systems Europe, 210-TA), human IL-1 β (R&D Systems Europe, 201-LB), TNF β (R&D Systems Europe, 211-TB), IL-17A (R&D Systems Europe, 317-ILB, poly(I:C) (Invivogen, tlrl-pic) or phorbol-12-myristate-acetate (PMA; P-8139) from Sigma Aldrich. Cytokine production by fibroblasts was assessed after incubation for 24 h without stimulation, or with TNF α , IL-1 β , IL-17A, poly(I:C) or phorbol-12-myristate-acetate (PMA) stimulation. IL-6 and IL-10 secretion was quantified with an ELISA kit (M9316 and M1910 - Sanquin). The specific antibodies used for detection on western blots were rabbit anti-NEMO (#sc-8330, Santa Cruz), mouse anti-I κ B α (#610690, BD Transduction Laboratories), rabbit mAb anti-phospho-IKK α / β (ser176/180) (#16A6, Cell Signaling), mouse

anti-IKK β (#AM8109a, Abgent), anti-ERK1/2 (#9102, Cell Signaling), anti-p-ERK1/2 (#9101, Cell Signaling), anti-p65 (#4764, Cell Signaling), anti-p-p65 (#3033, Cell Signaling), anti-JNK (#9252, Cell Signaling), anti-p-JNK (#9255, Cell Signaling), anti-p38 (#9212, Cell Signaling), anti-p-p38 (#9215, Cell Signaling), mouse anti- β -ACTIN (#013-24553, WAKO) and mouse anti-GAPDH (#sc-81545, Santa Cruz Biotechnology or #016-25523, WAKO) antibodies. Mouse, rabbit and goat secondary antibodies coupled to horseradish peroxidase (HRP) were obtained from Vector Laboratories or Amersham-Pharmacia. Signals were quantified with Image Studio Lite Software (Version 5.2.5; LI-COR).

Peripheral blood mononuclear cells (PBMCs) were isolated from the whole blood of a patient (P3) and from controls with Lymphoprep (Alere Technologies AS). For the cytokine secretion assay, PBMCs were stimulated with LPS (1 μ g/mL, Sigma) and IFN- γ (5000 U/mL, Peprotech) for 48 hours. The level of TNF α secretion was determined with the Bio-Plex MAGPIX system (Bio-Rad). For the intracellular staining of TNF α in CD14-positive monocytes, PBMCs were stimulated with LPS (100 ng/mL, Sigma) in the presence of monensin (BD) for 4 hours. Cells were stained with CD14-FITC (#11-0149-41, eBiosciences), fixed and permeabilized with Cytotfix-Cytoperm (BD), and then stained with anti-TNF α -PE antibody (#554513, BD). Cells were analyzed with a FACScalibur machine (BD).

References

1. Li H, and Durbin R. Fast and accurate short read alignment with Burrows-Wheeler transform. *Bioinformatics*. 2009;25(14):1754-60.
2. McKenna A, Hanna M, Banks E, Sivachenko A, Cibulskis K, Kernytsky A, et al. The Genome Analysis Toolkit: a MapReduce framework for analyzing next-generation DNA sequencing data. *Genome Res*. 2010;20(9):1297-303.
3. Li H, Handsaker B, Wysoker A, Fennell T, Ruan J, Homer N, et al. The Sequence Alignment/Map format and SAMtools. *Bioinformatics*. 2009;25(16):2078-9.

4. Martin M. Cutadapt removes adapter sequences from high-throughput sequencing reads. *EMBnetjournal*. 2011;17(1).
5. Dobin A, Davis CA, Schlesinger F, Drenkow J, Zaleski C, Jha S, et al. STAR: ultrafast universal RNA-seq aligner. *Bioinformatics*. 2013;29(1):15-21.
6. Garcia-Alcalde F, Okonechnikov K, Carbonell J, Cruz LM, Gotz S, Tarazona S, et al. Qualimap: evaluating next-generation sequencing alignment data. *Bioinformatics*. 2012;28(20):2678-9.
7. Smahi A, Courtois G, Vabres P, Yamaoka S, Heuertz S, Munnich A, et al. Genomic rearrangement in NEMO impairs NF-kappaB activation and is a cause of incontinentia pigmenti. The International Incontinentia Pigmenti (IP) Consortium. *Nature*. 2000;405(6785):466-72.
8. Nakagawa M, Taniguchi Y, Senda S, Takizawa N, Ichisaka T, Asano K, et al. A novel efficient feeder-free culture system for the derivation of human induced pluripotent stem cells. *Sci Rep*. 2014;4:3594.
9. Okita K, Yamakawa T, Matsumura Y, Sato Y, Amano N, Watanabe A, et al. An efficient nonviral method to generate integration-free human-induced pluripotent stem cells from cord blood and peripheral blood cells. *Stem Cells*. 2013;31(3):458-66.
10. Haruta M, Tomita Y, Yuno A, Matsumura K, Ikeda T, Takamatsu K, et al. TAP-deficient human iPS cell-derived myeloid cell lines as unlimited cell source for dendritic cell-like antigen-presenting cells. *Gene Ther*. 2013;20(5):504-13.
11. Eiraku M, Watanabe K, Matsuo-Takasaki M, Kawada M, Yonemura S, Matsumura M, et al. Self-organized formation of polarized cortical tissues from ESCs and its active manipulation by extrinsic signals. *Cell Stem Cell*. 2008;3(5):519-32.
12. Yoshida M, Kataoka N, Miyauchi K, Ohe K, Iida K, Yoshida S, et al. Rectifier of aberrant mRNA splicing recovers tRNA modification in familial dysautonomia. *Proc Natl Acad Sci U S A*. 2015;112(9):2764-9.
13. Ramaswami S, and Hayden MS. Electrophoretic mobility shift assay analysis of NF-kappaB DNA binding. *Methods Mol Biol*. 2015;1280:3-13.

Case Report

Rescue of recurrent deep intronic mutation underlying cell type-dependent quantitative NEMO deficiency.

Bertrand Boisson^{1,2,3@*}, Yoshitaka Honda^{4*}, Masahiko Ajiro^{5,6#}, Jacinta Bustamante^{1,2,3,7#},
Matthieu Bendavid^{1#}, Andrew R. Gennery^{8#}, Yuri Kawasaki⁹, Jose Ichishima⁹, Mitsujiro Osawa⁹,
Hiroshi Nihira⁴, Takeshi Shiba⁴, Takayuki Tanaka⁴, Maya Chrabieh^{2,3}, Benedetta Bigio¹, Hong
Hur¹⁰, Yuval Itan¹, Yupu Liang¹⁰, Satoshi Okada¹¹, Kazushi Izawa⁴, Ryuta Nishikomori⁴, Osamu
Ohara^{12,13}, Toshio Heike^{4,14}, Laurent Abel^{1,2,3}, Anne Puel^{1,2,3}, Megumu K. Saito^{9§},
Jean-Laurent Casanova^{1,2,3,15,16,\$,@}, Masatoshi Hagiwara^{5,6§} and Takahiro Yasumi^{4,\$@}

Case report

Kindred A:

The mother was diagnosed with incontinentia pigmenti at the age of one year, on the basis of pigmented skin lesions following Blaschko's lines. She had no relevant family history and there was no prior evidence of skin blistering or verruca-like lesions, and no dental abnormalities or other stigmata associated with incontinentia pigmenti. When she was seen again at the age of 19 years, the lack of a history of blistering or warty changes in the skin before the hyperpigmentation of the Blaschko's lines, and the normality of her teeth and nails led to a revision of the diagnosis to familial cutaneous amyloidosis. Skin biopsy showed orthokerotosis and minimal focal acanthosis, with a light superficial perivascular lymphocytic infiltrate and melanophages scattered throughout the upper dermis. There was no active inflammation, atopia or neoplasia. Specific amyloid staining was negative.

P1, the first male child, was born at 36 weeks of gestation, by cesarean section because of growth retardation. Birth weight was on the 0.4th centile. The child was initially well, but had developed liver dysfunction by day 9, and, on day 12, was noted to be unwell, with mottled skin. Despite the absence of fever or detectable infection, C-reactive protein (CRP) concentration had risen to 105 mg/L (normal (0-5)) and antibiotic treatment was initiated. Spinal CSF examination was normal. The following day, clinical evidence of necrotizing enterocolitis was detected. *Klebsiella oxytoca* was isolated from blood culture. Despite appropriate antibiotic treatment, the child developed a brain infection and died on day 21. His temperature remained low [34.5-35°C] despite infection, except for two short peaks [up to 39°C]. Maximum white blood cell count was $32.6 \times 10^9/L$, with evidence of toxic neutrophilia. Lymphocyte count was normal. *Klebsiella oxytoca* was subsequently grown from spinal cerebrospinal fluid after the death of the child, and

post mortem showed diffuse necrotic foci throughout the brain and liver, but the gut appeared normal, with no evidence of necrotizing enterocolitis.

P2, the second male child, was born at 37 weeks of gestation by elective cesarean section. The pregnancy was normal. The child's weight was below the 0.4th centile at birth. On day 2, he became unwell with suspected sepsis. On examination, no abnormalities were observed other than mild jaundice. In particular, P2 had no physical abnormalities, with no dysmorphic features or skin rashes, in particular. P2 underwent a full septic screen (temperature, CRP, blood culture) and was treated for 10 days with IV antibiotics (cefotaxime, amoxicillin, gentamicin). Initial investigations revealed a normal whole-blood cell count, electrolyte levels and liver function test results. IgM and IgG levels were normal, but no IgA was detected. Lymphocyte marker levels were normal, with the exception of a slightly high CD8 count. Neutrophil markers (CD35, CD16, CD18) were all expressed normally, and the neutrophil oxidative burst was normal. Antibiotic prophylaxis with cotrimoxazole was initiated. At the age of four months, P2 presented gram-negative *Enterobacter* septicemia, which was treated with intravenous antibiotics. Small round viruses were isolated from his feces. Upper and lower intestine biopsy results were normal. The patient's immunoglobulin levels fell and he responded poorly to three doses of tetanus and *Haemophilus influenzae b* (Hib) immunization (Tet 0.02 IU/mL (0.1-10), Hib <0.11 mg/L (1.0-20)). Intravenous immunoglobulin replacement was initiated. The patient's T-cell response to mitogens was normal at this time, and the results of ADA and PNP studies were normal. At six months of age, P2 was readmitted due to weight loss and total parenteral nutrition (TPN) was initiated. Astrovirus and *Candida albicans* were isolated from stools, and *Candida* plaques were observed in the esophagus on endoscopy. A duodenal biopsy specimen tested positive for HHV6. The patient had *Klebsiella oxytoca* septicemia associated with neutropenia, which was treated with cefotaxime and gentamicin, but

no increase in CRP concentration (<15) or temperature was observed. Long-term TPN, with continual bacterial and fungal prophylaxis and IVIG treatment was instigated. At the age of nine months, P2 developed respiratory syncytial virus (RSV) bronchiolitis. Despite treatment with nebulized ribavirin, and intravenous and nebulized RSV-specific immunoglobulins, P2's vital signs rapidly deteriorated and he required mechanical ventilation. A lung biopsy specimen was strongly positive for RSV and no improvement was observed in the patient's condition. The decision was made to withdraw treatment, after which the patient died. On post-mortem analysis, he was found to have a small but normally formed thymus and no lymph nodes. RSV was isolated from the lung and micro-abscesses were observed, in which *Aspergillus* was identified by histology. Lymphocyte subset analysis at birth showed high T-cell counts (CD4 and CD8) but B-cell counts in the normal range. Over the following months, this situation reversed and, at the time of P2's final admission to hospital, he had only 385 CD3⁺ lymphocytes (1,700-3,600) and 100 CD8⁺ cells (1,700-2,800) per mL, but 2,292 B cells (500-1,500). He had NK-cell lymphopenia, which normalized by the time of his final admission. T-cell receptor V β analysis showed a normal distribution, consistent with a polyclonal population of lymphocytes. P2 also had a normal TCR $\alpha\beta/\gamma\delta$ ratio and a normal ratio of naïve to memory CD3⁺ T cells. Lymphocyte proliferation in response to PHA, PMA, and α -CD3+IL-2 was consistently weaker than that for a healthy control.

Kindred B:

P3 was the third son of four siblings born at term after noneventful pregnancies to healthy, non-consanguineous Japanese parents. He became ill at the age of 15 days, with mild fever and a generalized reticular rash. He had normal straight hair and eyebrows. On initial evaluation, WBC count was high, at 13,800 x10⁹ cells/L (67% neutrophils, 28% lymphocytes, 2% eosinophils, and 3% monocytes) and platelet levels were slightly low, at 163 x10⁹/L. CRP levels were high, at 65.7

mg/L, together with lactate dehydrogenase (5,161 U/L) and ferritin (75,093 µg/L) levels. CSF analysis revealed no pleocytosis, but *Escherichia coli* was detected in peripheral blood and CSF cultures. The patient was saved by treatment with IV antibiotics and continuous hemodiafiltration but suffered severe encephalomalacia as a sequel. The reticular rash slowly became less marked, over a period of several months. At four months of age, IgG levels dropped to 1440 mg/L, and immunoglobulin supplementation was started. At this point, IgM and IgA levels were 140 mg/L and 90 mg/L, respectively. At five months of age, the patient began to suffer from diarrhea, followed by coughing and tachypnea. Chest CT examination revealed diffuse interstitial pneumonia. The patient was transferred to Kyoto University Hospital because he was suspected to have an underlying immunodeficiency. On arrival, his WBC count was high (16,800/µL) with marked eosinophilia (33% of WBC) and lymphopenia (14% of WBC). CRP concentration was high, at 13.0 mg/L. Immunophenotyping revealed that CD3⁺ cell counts were low, at 967/µL, but B-cell counts were normal (1165 /µL). CD3⁻CD56⁺CD16⁺ NK cells were present in only very small numbers. *Streptrophomonas maltophilia* was detected in blood culture, whereas Coxsackievirus type B5 and *Pneumocystis jirovecii* were detected in bronchopulmonary lavage fluid. Intensive treatment with a combination of antibiotics that had proved effective *in vitro* was not effective in the patient, who died from respiratory failure at six months of age. The proliferative response of lymphocytes to PHA and ConA was weak. TNFα production by peripheral blood mononuclear cells in response to LPS and IFNγ was severely impaired (**Supplementary Fig. 11H**). These findings are consistent with the weak intracellular staining of TNFα observed in monocytes in response to LPS stimulation (**Supplementary Fig. 11I**). Conventional sequencing of the exons and exon-intron boundaries of the *IKBKG*, *NFKB1A*, *IRAK4*, and *MyD88* genes identified no pathogenic variant.